

## DESIGN OF A NATURAL CIRCULATION CIRCUIT FOR 85 MW STEAM BOILER

by

**Konstantin A. PLESHANOV<sup>a\*</sup>, Ekaterina G. KHLYST<sup>b</sup>,  
Mikhail N. ZAICHENKO<sup>a</sup>, and Kirill V. STERKHOV<sup>a</sup>**

<sup>a</sup> Radioengineering and Electronics,  
Moscow State University of Information Technologies, Moscow, Russia

<sup>b</sup> Moscow Power Engineering Institute,  
Russia National Research University, Moscow, Russia

Original scientific paper  
<https://doi.org/10.2298/TSCI161005320P>

*The paper describes research and design of fluidized bed steam boiler natural circulation circuit. The capacity of the drum boiler is 85 MW, superheated steam pressure is 98 bar. There are two variants research results of the designed circulation circuit. The first circulation circuit variant was designed as a complex circuit with a common downcomers and risers for the boiler evaporating screen. In the second variant the flow is separately supplied to and discharged from the evaporator that is divided into independent sections. We have researched and described the influence of heat absorption inequality on the furnace evaporation pads using the Boiler Designer software. We also have calculated main characteristics of the two-phase flow in the evaporation pads and evaluated reliability of the natural circulation. The circulation circuit is optimized from point of view of reliability and metal expenses. Results demonstrate that the specific quantity of metal of complex and simple circuit variants is approximately the same with equal reliability.*

Key words: *steam, drum, boiler, natural circulation, Boiler Designer software, evaporator, reliability, circulation circuit, calculation, optimization*

### Introduction

Ensuring reliable operation of the evaporator in a steam boiler is an important task. Performing this task requires two conditions to be provided: reliable circulation to cool the evaporator and the needed tube temperature regime (to avoid critical heat flux – CHF) [1]. Directed flow motion is achieved by the design of non-heated circulation circuit tubes and the changes in the two-phase flow physical properties during the heating of heat-exchange surface. The paper offers criteria and approaches that make it possible to design and optimize the natural circulation circuit design from the perspective of simplicity and minimizing the metal mass while providing reliable circulation. The work of two circulation circuits has been design and described in the paper: complex circuit with common flow input and output and numerous evaporators with independent flow input and output.

The circulation circuit was developed and researched for a drum-type boiler, fig. 1, with steam capacity of 33.33 kg/s, superheated steam pressure of 98 bar and superheated steam

\* Corresponding author, e-mail: [energo\\_01@yahoo.com](mailto:energo_01@yahoo.com)

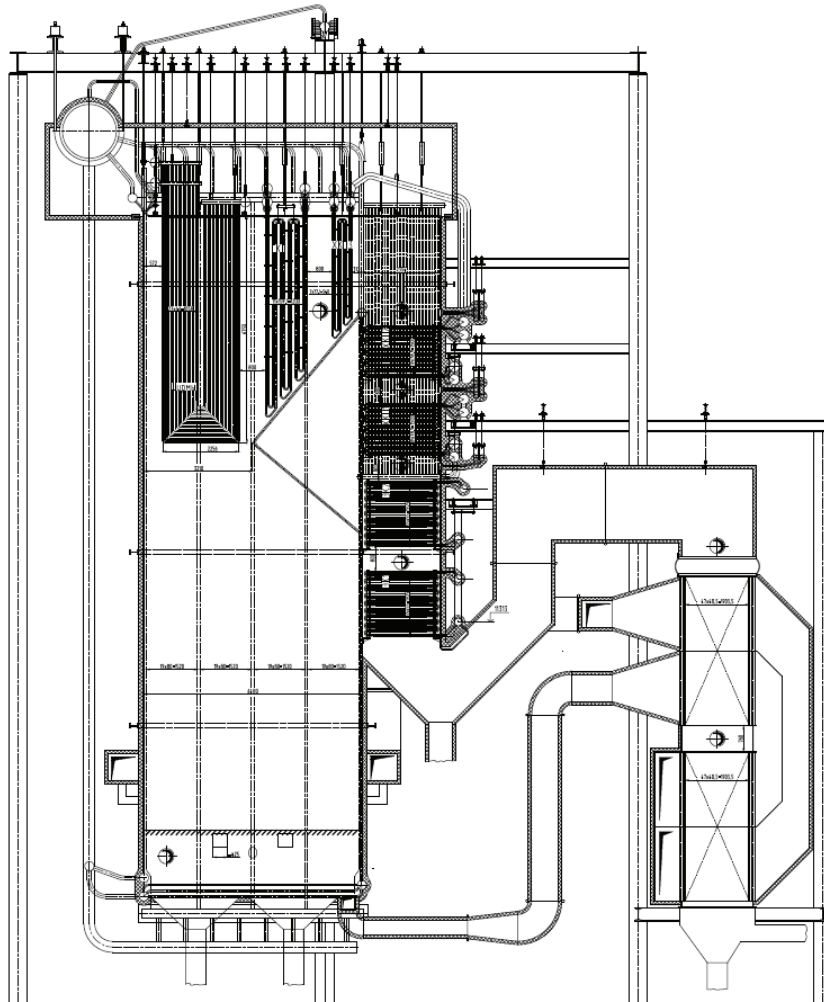


Figure 1. The 85 MW steam boiler

temperature of 540 °C. The detailed process of biofuel fluidized bed boiler design and its results are provided in [2, 3].

Research target: design the diagram and construction of the circulation circuit.

Tasks needed to achieve the following target.

- Develop an approach to the optimization of the piping system of a natural circulation circuit.
- Choose the optimization criteria, necessary and sufficient criteria for the development of the optimal circulation circuit design.
- Study the influence of unequal heat absorption on the performance of a natural circulation circuit.
- Identify the optimal design variant of the evaporation system.

The main instructive materials [1] to design a circulation circuit do not provide clear instructions for the design algorithm and the criteria of the result optimality. Hydraulic design of boiler units standard method suggests to choose constructive characteristics of the circulation circuit depending on the working two-phase flow pressure. The design is considered to be

complete when a constructive solution meets the reliability requirements in terms of natural circulation stagnation and inverting and in terms of required tube temperature regime. This can be explained with the fact that previously all time-consuming iterational circulation calculations were performed manually.

Natural circulation circuit calculation is based on fact, that total pressure gradient in system drum-downcomers-evaporator-risers-drum equals 0. The local pressure changes  $\Delta P$  in single- or two-phase flow may be represented by:

$$\Delta P = \Delta P_f + \Delta P_l \pm \Delta P_g + \Delta P_a \quad (1)$$

where  $\Delta P$  is the pressure changes from local wall friction losses,  $\Delta P_l$  – the pressure changes from local losses (bends, fittings),  $\Delta P_g$  – the hydrostatic pressure changes, and  $\Delta P_a$  – the pressure changes from flow acceleration. Basic equations for pressure changes are presented in tab. 1 from [1].

**Table 1. Basic equations for pressure changes [Pa]**

Single-phase flow	eq.	Two-phase flow	eq.
$\Delta P_f = \frac{\lambda_0 l (\rho w)^2}{2 \bar{\rho}}$	(2)	$\Delta P_f = \frac{\lambda_0 l (\rho w)^2}{2 \rho'} \left[ 1 + \bar{x} \bar{\psi} \left( \frac{\rho'}{\rho''} - 1 \right) \right]$	(3)
$\Delta P_l = \zeta \frac{(\rho w)^2}{2 \rho}$	(4)	$\Delta P_l = \zeta' \frac{(\rho w)^2}{2 \rho'} \left[ 1 + x \left( \frac{\rho'}{\rho''} - 1 \right) \right]$	(5)
$\Delta P_g = \pm h \bar{\rho} g$	(6)	$\Delta P_g = \pm h \left[ \rho' - \bar{\varphi} (\rho' - \rho'') \right] g$	(7)
$\Delta P_a = (\rho w)^2 \left( \frac{1}{\rho_2} - \frac{1}{\rho_1} \right)$	(8)	$\Delta P_a = \frac{(\rho w)^2}{\rho'} \left( \frac{\rho'}{\rho''} - 1 \right) (x_2 - x_1)$	(9)

The main circulation dysfunctions and the criterias which allow to identify them according to [1] are described. Circulation stagnation is slow upward or downward motion of water in the pipe combined with the upward motion of steam. Steam bubbles can stagnate in certain areas (bending points, wending points, branch connections). The amount of supply water for the evaporator is usually equal to the amount of evaporated water. Circulation inverting happens in the case of steam lock caused by the accumulation of steam that can not overcome the dynamic influence of the downcoming water and can not exit to the risers header or drum. In both cases of circulation dysfunctions the temperature of the wall will rise in the areas where steam is accumulated and does not cool the metal sufficiently. In steam boilers [4] this may lead to the exceeding of the temperature limit of the tube metal and later to its destruction due to scaling or structural changes. Proper temperature regime of the tube operation is also provided by absence of CHF [1, 5]. Circulation stagnation and inverting are evaluated by stability coefficients – the ratio between stagnation or inverting head and effective head. If these ratios are over 1.1 the system is considered to be reliable.

Following values are used to calculate the natural circulation reliability in according to [1]: dynamic head,  $S_d$  in eq. (10), effective head,  $S$  in eq. (11), stagnation head,  $S_s$ , inverting head,  $S_p$ , hydraulic pressure changes the  $\Delta P$ . Stagnation head and inverting head were calculated in accordance with [1]. They are the indicators of circulation stability limits.

Dynamic head [Pa] is the differential of hydrostatic pressure changes in the riser and downcomer parts of the circulation circuit:

$$S_d = \bar{\varphi}(\rho' - \rho'')hg \quad (10)$$

Effective head is the differential of the dynamic head and hydraulic pressure changes in the riser tubes:

$$S = S_d - \Delta P \quad (11)$$

Stability coefficients of stagnation and inverting are equal the ratio between the head of stagnation or inverting to the effective head:

$$\frac{S_s}{S} \quad \text{and} \quad \frac{S_i}{S} \quad (12)$$

Most designers [6, 7] use the method described in [1]. The negative aspect of this approach consists of the fact that risers and downcomers may have more complicated configuration and cumbersome construction due to the absence of optimization.

There are two possible variants of the circulation circuit configuration. Complex circulation circuit with common downcomers and risers, fig. 2(a), is often used in hot gases recovery boilers [8, 9] and steam boilers designed in the EU countries [10, 11]. Simple circuits with independent flow discharge and supply, fig. 2(b), with separate furnace evaporation pads are more often used in Russia [6, 12]. Complex circuit is easier in terms of structural design compared to the simple circuit. It does not cram up the boiler so much and the tube length is shorter. Many engineers and researchers believe that using the simple circuit provides better reliability with more unequal heat absorption in the boiler furnace [6, 7]. Each of the boiler manufacturers prefers the more technologically familiar variant.

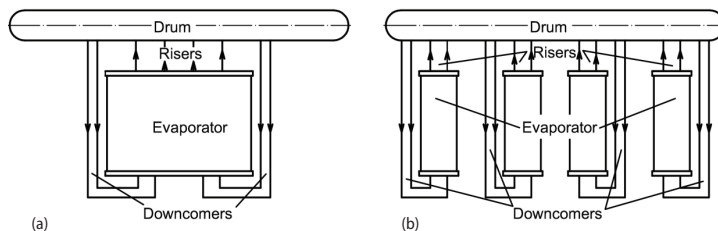


Figure 2. Circulation circuit; (a) – complex, (b) – simple

### System description

Construction of the 85 MW steam boiler walls consists of four pads each. In complex circulation circuits the pads of each wall are completed into one supplying and collecting headers, fig. 3. In simple

circulation circuits they have independent headers that provide independent supply and exhaust of the flow.

The performance of an evaporating element and the two-phase flow rate depends on its heat absorption. Generally, specific consumption of a given tube part depends on its location in the furnace and is calculated with the formula:

$$q_t = \eta_{\text{wall}} \eta_{\text{wide}} \eta_{\text{el}} \eta_{\text{high}} \bar{q} \quad (13)$$

Coefficient of heat absorption inequality  $\eta$  is the ratio of densi heat flux of a tube to the density of heat flux element:

- $\eta_{\text{wall}}$  – by furnace walls,
- $\eta_{\text{wide}}$  – by furnace wall width,
- $\eta_{\text{el}}$  – by element (of an evaporation pad), and
- $\eta_{\text{high}}$  – by furnace height.

For fluidized-bed boilers. According to the recommendations [1], maximum and minimum coefficients of heat absorption inequality width furnace elements is the product of and equals 1.3 and 0.5 for the complex circulation circuit and  $1.1 \cdot 1.1 = 1.21$  and  $0.9 \cdot 0.7 = 0.63$  for simple circuits, in cases when four pads are located on one furnace wall. In this paper an extended range of heat absorption inequality (0.2-1.5) was used to detailed investigation.

The changes in heat absorption inequality coefficient furnace height for different areas are provided in tab. 2.

Computer model that was used to study the performance of the natural circulation circuit was created with Boiler Designer software [8, 9]. The evaporator was divided into four areas furnace width and height according to [1] (dense bed, splashing region, platen area, and aerodynamic nose area) as shown on fig. 4. This enabled proper calculation of how each sector influences the performance of the whole circuit.

### Calculation results

Here the results of calculation study of the performance of evaporation tubes with the worst thermohydraulic conditions are shown. When the pressure is 110 bar, the inverting head is lower than the stagnation head, so the stability of natural circulation will be defined by inverting. The study of the furnace height heat absorption inequality influence on the evaporator operation has shown that the maximum heat absorption on the initial part is the worst variant. At the same time, the inverting stability coefficient for the *worst tube* of the side wall provided in tab. 3 is 30% less compared to design case 1 and 15% less compared to design case 2. This happens because of the inverting head decrease and effective head increase caused by the more intensive increase of steam quality. It should be separately pointed that the flow in the circulation circuit increased 5% and the steam quality between the 1 and 3 design cases decreased. This is not typical for natural circulation, because generally when the flow increased and the steam quality decreased the reliability of the system increases.

Further research used variant 3 with the maximum heat absorption on the initial part of the evaporator in the furnace. Initial part of the evaporator is located above the fluidized bed close to the secondary air inlet. When biofuel is burned in the fluidized bed the largest heat emission is registered in the freeboard [13]. This is conditioned by the high volatile content in the fuel that is mostly burned above the fluidized bed.

The parameters of non-heated circulation tubes used for the design are provided in tab. 4. It shows that as the tube diameter and thickness increase the mass of 1 running meter of the tube rises as well due to the larger amount of metal needed to produce it. Consequently, the

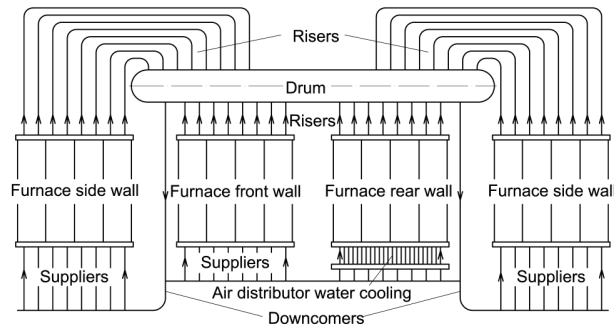


Figure 3. Complex circulation circuit of an 85 MW steam boiler

Table 2. Changes in heat absorption inequality coefficient by furnace height

Design case	Relative height of the area in the furnace			
	0.27	0.44	0.69	0.9
1	1.6	1	0.78	0.62
2	0.6	1.6	1.18	0.62
3	0.6	0.84	1	1.56

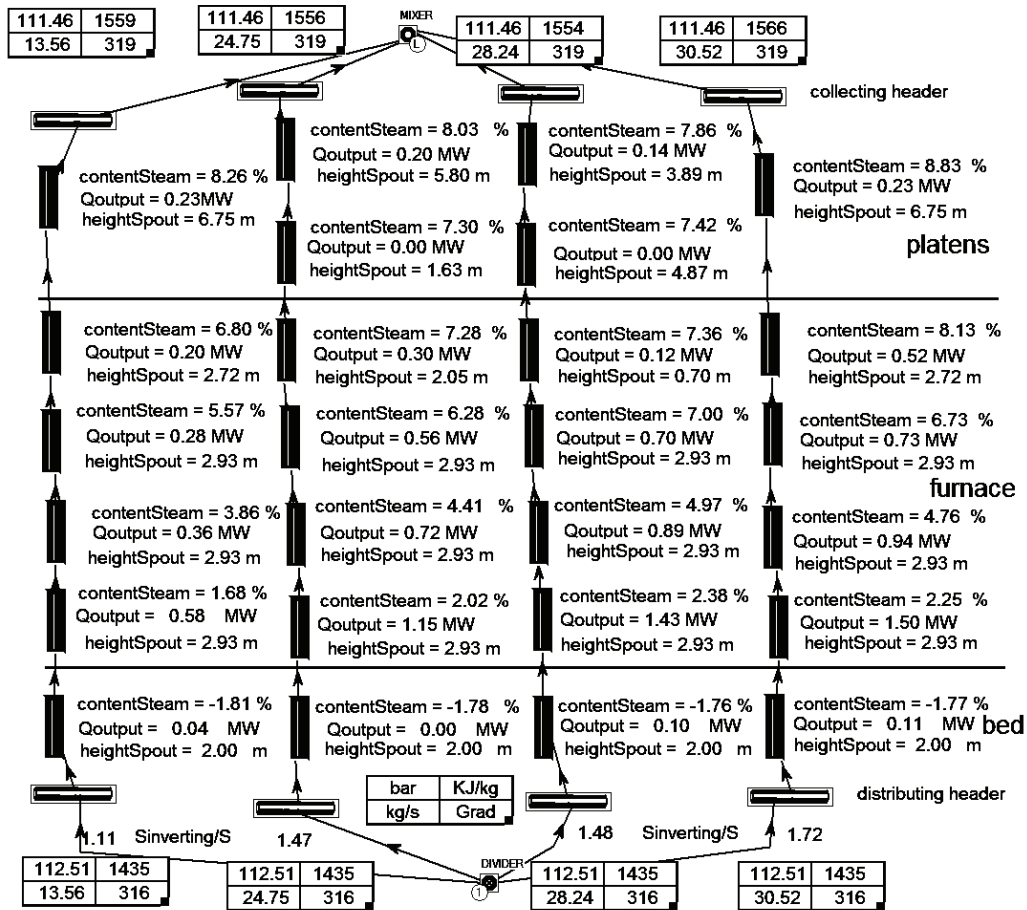


Figure 4. Evaporator divided by sections

Table 3. Calculation results of natural circulation side wall furnace height for different heat absorption distribution

Design case (tab. 1)	1	2	3
Two-phase flow [kgs <sup>-1</sup> ]	86.22	89.42	92.12
Outlet steam quality [%]	8.75	8.49	8.27
Dynamic head [bar]	0.27	0.2995	0.3225
Hydraulic pressure loss [mbar]	4.95	5.45	5.8
Effective head [bar]	2.205	2.45	2.645
Stagnation head [bar]	5.655	6.215	6.925
Inverting head [bar]	4.835	4.545	4.27
Stagnation stability coefficient	2.6	2.5	2.6
Inverting stability coefficient	2.2	1.8	1.6

Table 4. Parameters of the non-heated tubes of the natural circulation circuit

Circuit section	Diameter × thickness [mm]	Mass of 1 m of tube [kg]
Downcomer	168 × 12	49.34
	219 × 13	70.66
	273 × 16	108.64
	325 × 20	161.13
	377 × 22	206.35
Supply and riser	465 × 25	264.87
	89 × 6	12.56
	108 × 7	17.84
	121 × 8	23.84
	133 × 9	29.42
	168 × 10	41.69
	194 × 11	53.12

increase in the size of the used tubes leads to the increase of the specific amount of metal of the boiler.

While the flow remains the same, fig. 5, it can be seen that the inverting stability coefficient is 40-50% less than that in case of stagnation. This can be explained by the properties of water and steam at the pressure of 110 bar. Inverting head is lower than the stagnation head, so the reliability of circuit operation will be conditioned by the fact of circulation inverting.

Dates of the fig. 5 show that in the low flow areas tube size changes do not result in significant changes of the stability coefficients. Downcomers of  $168 \times 12$  mm and  $219 \times 13$  mm combined with risers has not provided system reliability. The largest rise of flow has been achieved with changing the risers tube when downcomers tubes were  $465 \times 25$  mm. In this case both the stagnation stability coefficient and the inverting stability coefficient exceeded the minimal value of 1.1 in according to [1], which was achieved with circuit flow above 280 kg/s.

The increase in the mass of non-heated tubes of the natural circulation circuit does not always lead to the increase in the system reliability, fig. 6. It is necessary to develop an approach that would enable to connect system performance reliability and metal mass. As the typical size of non-heated tubes grows, the dependence of specific amount of metal gradient on the flow is changes.

In the small flow rate 140-280 kg/s the riser diameter increase did not promote larger flow in the system. In this flow rate the increase of downcomers tube typical sizes is more efficient. As the typical size of the tubes is increased this tendency is changed. In the area of 280-470 kg/s changes of downcomers and risers tubes have led to comparable increases of flow. In the flow rate above 470 kg/s the risers but not the downcomers ones become the limiting factor. This is demonstrated with the *I* curve of maximum flow increase with minimal metal mass, fig. 6. Such flow changes of flow dependence on the non-heated tube size indicates that different sections of the system is a limiting factor.

Circulation diagram is the traditional result of natural circulation calculation [1, 5]. Figure 7 demonstrates such a diagram for tubes described in tab. 4. This figure shows zones of different metal mass with 5 tonne step. The flow area of 280-470 kg/s that provides reliability gets into the II and III zones with the metal mass of 10-15 t and 15-20 t, respectively. Larger

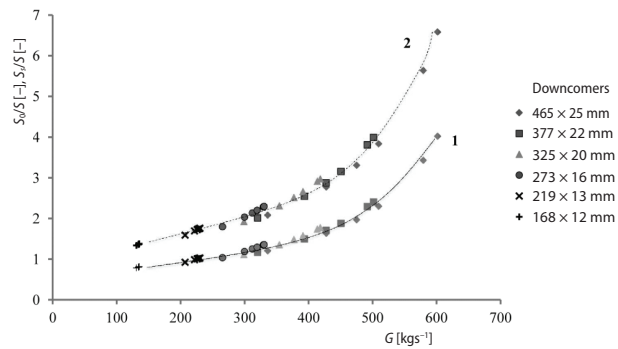


**Figure 5. Stagnation and inverting stability coefficients;**  
 1 – inverting stability coefficient, 2 – stagnation stability coefficient

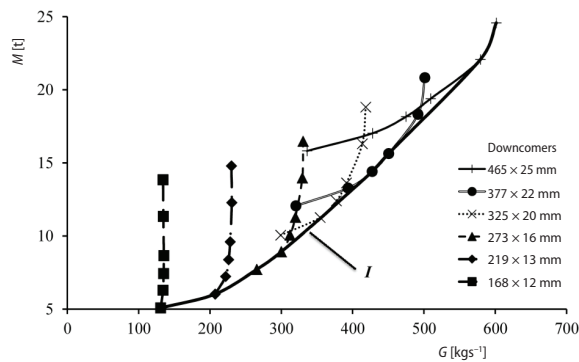


**Figure 6. Non-heated tube metal mass of the circulation circuit;**  
 I – area of minimal metal mass with maximum flow

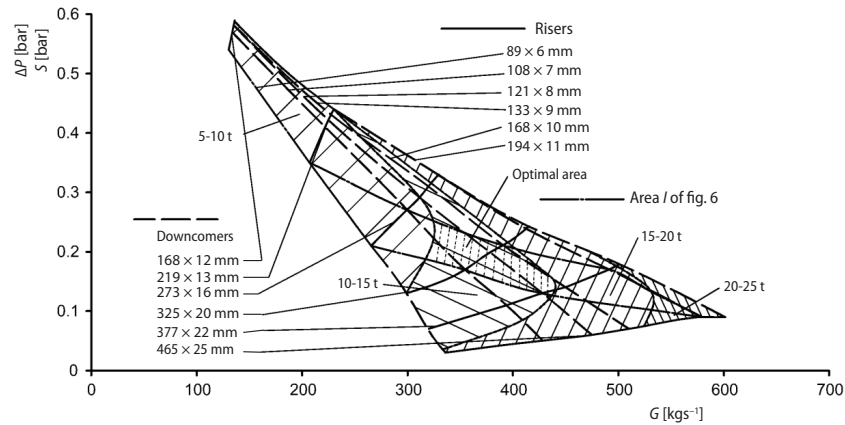


Figure 7. Complex circuit circulation diagram

flow will result the increase of metal mass accompanied with excess reliability. As the final result, the variant with system flow below 280 kg/s was turned down as it does not provide reliable system performance, alongside with the variant of above 470 kg/s that leads to excessive metal expenses.

The optimal solution for the presented areas will belong to the curve of maximum flow increase with minimal metal mass. Circulation circuit parameters in the *II* and *III* areas with metal mass of 10-20 t featured in tab. 5.

The tubes demonstrated in tab. 5 were further used to study the influence of heat absorption inequality furnace width on the circulation circuit operation. Heat absorption coefficient furnace width equals 0.2, 0.5, 1, 1.2, 1.3, and 1.5 due to the reasons mentioned previously.

Consequently the minimally acceptable inverting stability coefficient of 1.1 according to [1] was registered for downcomers 325 × 20 [mm] and risers 121 × 8 [mm]. The indicated value of was watched when  $\eta_{\text{wall}} = 0.5$ . In practice, the reduction of  $\eta_{\text{wall}}$  to 0.2-0.5 is improbable for a fluidized bed boiler. This makes it possible to conclude that this system is workable. As a result, variant 2 from tab. 5 was chosen as the optimal one in terms of ensuring reliable operation of a natural circulation circuit and minimal metal mass.

Pressure changes from flow acceleration and local losses usually do not exceed 10% of the total pressure changes, and the influence of such losses on the two-phase flow in the circulation circuit is insignificant. Evaporator resistance is mostly combined of the hydrostatic pressure changes and friction pressure changes. When the differential pressure between the evaporator tubes is equal, this leads to reduced flow due to the increase in the hydrostatic pressure in the evaporator. This can be seen on fig. 8(a) – the area of large flow 20-35 kg/s and heat absorption 3-4 MW. As the heat absorption is reduced to 1 MW, fig. 8(a), the steam quality increases. This will lead to significant reduction of flow to 3 kg/s, fig. 8(b). The increase of steam

Table 5. Operation parameters of the optimal circulation circuit design

$N_{\text{e}}$	Downcomers tubes diameter × thickness [mm]	Supply and risers tubes diameter × thickness [mm]	Flow [ $\text{t}\cdot\text{h}^{-1}$ ]	$S_i/S$	$M$ [t]
1	325 × 20	108 × 7	1290	1.3	11.5
2	325 × 20	121 × 8	1355	1.5	12.5
3	377 × 22	121 × 8	1540	1.7	14.5
4	377 × 22	133 × 9	1620	1.8	15.5



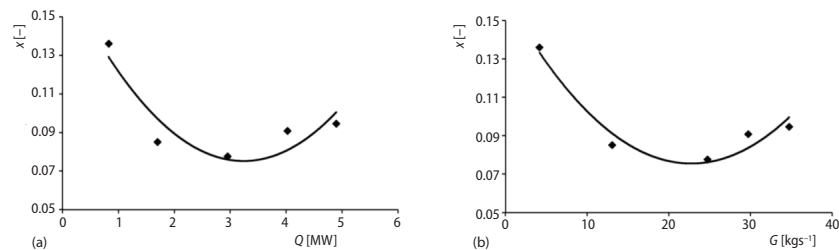


**Figure 8. Changes of steam quality depending on the evaporator operation regime**

quality at low flow rate is explained by the fact that the amount of generated steam is so low that the change in static pressure grows substantially. When the differential pressure between the inlet and outlet headers is constant, the friction resistance is inevitable decreased, which is only possible if the flow in the system is reduced.

Small heat output, fig. 8(a), cases small flow, fig. 8(b), and steam quality increase in the natural circulation circuit. It usually occurs in the regimes of stagnation or inverting. The  $S_i/S = 0.9$  only at  $\eta_{\text{wall}} = 0.2$  which does not occur in practice and steam quality totaled 13%. When heat absorption is increased a large amount of steam is generated in the evaporator. Large dynamic head caused by higher steam generation can drive a bigger flow through the circuit.

The CHF test has shown that the heat current density totaled  $80 \text{ kW/m}^2$ . This is lower than  $465 \text{ kW/m}^2$ , so in according to [1] at the two-phase flow pressure of 110 bar there will be no CHF. Conducted calculations show that the performance of a complex natural circulation circuit with downcomers  $325 \times 20 \text{ [mm]}$  and risers  $121 \times 8 \text{ [mm]}$  will be reliable.

An alternative solution to the complex natural circulation circuit shown in fig. 2(a) is the design of the simple circuits with independent two-phase flow input and output to each evaporator pad, fig. 2(b). In general, the sequence of actions and the nature of the calculated dependencies are similar both for the complex and the simple circuits. After the analysis of the designs of the simple natural circulation circuits design 1 was chosen as the most optimal. This design has one downcomer  $121 \times 8 \text{ mm}$  and two risers  $108 \times 7 \text{ mm}$ . Using only one downcomer contradicts with the recommendations [1], although it has often been used in practice in boilers with superheated steam pressure of 100-140 bar [12]. The resulting metal content of the circulation system that consists of simple circuits totaled 11.5 t. With  $\eta_{\text{wall}} = 0.5$  the inverting stability coefficient of the *worst tube*  $S_i/S$  amounted to 1.11.

Calculations demonstrate that the metal mass of complex and simple circuits differs 8%. On the one hand, the complex circuit has mildly larger mass of 12.5 t, but the drum design is simplified due to the smaller number of two-phase flow outlet nozzles. Tube routing also becomes easier. As a result, the manufacturing expenses for the circulation circuit will be practically the same.

## Conclusions

- Identifying the optimal design of a circulation circuit requires the study of circuit operation reliability and the mass of the needed metal.
- One necessary criteria of a circulation circuit is the stagnation and inverting stability coefficient in the *worst tube* should be above 1.1. The sufficient criteria for a lightweight design is finding the solution in the area that provides minimal metal mass with reliable system operation.



- [6] Belyakov, I. I., Experience Gained from the Operation of a Drum Boiler for a Pressure of 18.5 MPa, *Thermal Engineering*, 54 (2007), 7, pp. 572-577
- [7] Dvoinishnikov, V. A., *et al.*, The Substantiation and Choice of Basic Solutions on the E-160-3.9-440 Boiler for the AO MOSENERGO State Power Station no. 1 (GES-1), *Thermal Engineering*, 50 (2003), 12, pp. 994-1001
- [8] Roslyakov, P. V., *et al.*, A Study of Natural Circulation in the Evaporator of a Horizontal-Tube Heat Recovery Steam Generator, *Thermal Engineering*, 67 (2014), 7, pp. 465-472
- [9] Pleshanov, K. A., *et al.*, Calculating the Dynamic Characteristics of a Boiler-Utilizer at the Novogor'kovskaya Heat and Electric Power Plant, *Power Technology and Engineering*, 49 (2015), 3, pp. 206-211
- [10] Bolhar-Nordenkamp, M., *et al.*, Combustion of Clean Biomass at High Steam Parameters of 540 °C Results From a New 120 MW<sub>TH</sub> Unit, *Proceedings*, 18<sup>th</sup> European Biomass Conference, Florence, Italy, Vol. 1, 2010
- [11] Vainikka, P., *et al.*, Trace Elements Found in the Fuel and in-Furnace Fine Particles Collected From 80 MW BFB Combusting Solid Recovered Fuel, *Fuel Processing Technology*, 105 (2013), pp. 202-211
- [12] Roslyakov, P. V., *et al.*, Studying the Possibility of Separate and Joint Combustion of Estonian Shales and Oil Shale Retort Gas at Thermal Power Plants, *Thermal Engineering*, 62 (2015), 10, pp. 691-702
- [13] Scala, F., Salatino, P., Modelling Fluidized Bed Combustion of High-Volatile Solid Fuels, *Chemical Engineering Science*, 57 (2002), 7, pp. 1175-1196

